

# Numerical Investigations on Detectability of Crack by Contactless $j_C$ -Measurement Method<sup>\*)</sup>

Teruou TAKAYAMA, Atsushi KAMITANI and Hiroaki NAKAMURA<sup>1)</sup>

*Yamagata University, 4-3-16 Jyohnan, Yonezawa, Yamagata 992-8510, Japan*

<sup>1)</sup>*National Institute for Fusion Science, 322-6 Oroshi-cho, Toki 509-5292, Japan*

(Received 7 December 2012 / Accepted 22 February 2013)

The inductive method for measuring the critical current density  $j_C$  and detecting the crack in a high-temperature superconducting (HTS) film have been investigated numerically. To this end, a numerical code has been developed for analyzing the shielding current density in the film with a crack. The results of computations show that the accuracy of the inductive method is degraded remarkably due to the crack. Specifically, it is found that, if the orthographic projection of the coil overlaps with the crack, the value of measured  $j_C$  decreases. This is mainly because the spatial distribution of the shielding current density becomes asymmetry. In conclusion, the crack size and position can be accurately detected by measuring the  $j_C$ -distribution in the HTS film.

© 2013 The Japan Society of Plasma Science and Nuclear Fusion Research

Keywords: critical current density, crack detection, high-temperature superconductor, inductive method, numerical simulation

DOI: 10.1585/pfr.8.2401025

## 1. Introduction

As is well known, a high-temperature superconductors (HTSs) are used for developing various devices and systems such as nuclear fusion reactor, flywheel, and MRI, and they are characterized by some parameters. In particular, a critical current density  $j_C$  is one of the most important parameters, and it is important to measure the value of  $j_C$  accurately.

The standard four-probe method [1] has been generally used for measuring  $j_C$ . In the method, electrodes are deposited with a silver paste to decrease the measurement error. After a large current source flows in an HTS sample,  $j_C$  can be evaluated accurately from nonlinear  $V$ - $I$  characteristics. However, HTS characteristics may be degraded because of a heat generated between the electrodes and the sample. As a result, the process may lead to the destruction of a sample surface or to the degradation of superconducting characteristics. For this reason, contactless methods have been so far desired for measuring  $j_C$ .

As a contactless method for measuring  $j_C$ , Claassen *et al.* have proposed the inductive method [2]. By applying an ac current to a small coil placed just above an HTS film, they monitored a harmonic voltage induced in the coil. They found that, only when a coil current exceeds a threshold current  $I_T$ , the third-harmonic voltage develops suddenly. They conclude that  $j_C$  can be evaluated from the threshold current. In contrast to this, Mawatari *et al.* elucidated the inductive method on the basis of the critical state model [3]. From their results, they derived a

theoretical formula between  $j_C$  and  $I_T$ . In addition, they found that the theoretical curve shows an excellent agreement with the experimental one. In this way, the scientific basis of the inductive method was theoretically justified. Incidentally, this method has been successfully employed as the measurement of the  $j_C$ -distributions the detection of a crack [4].

In the previous study, a numerical code was developed for analyzing the time evolution of a shielding current density in an HTS film with crack [5]. By using the code, the inductive method was reproduced numerically. The results of computations showed that, although the threshold current  $I_T$  decreases due to the crack, its value does not necessarily decrease for the case with a small crack size. In fact, the accuracy is not degraded when the inner radius of the coil contains the crack of the film. For this reason, we conclude that the smallest possible inner radius is preferable to detect the crack.

The purpose of the present study is to simulate the inductive method for the case with crack containing in the HTS film, and we investigate the applicability of the detection of the crack size and position.

## 2. Governing Equation

In Fig. 1, we show a schematic view of an inductive method. A small  $M$ -turn coil is placed just above a rectangle-shaped HTS film of the length  $a$  and the thickness  $b$ , and an ac current  $I(t) = I_0 \sin 2\pi ft$  flows in it. Furthermore, the square cross-section of the film is denoted by  $\Omega$ , and an outer boundary of  $\Omega$  is expressed by  $C_0$ . Furthermore, we assume that a crack exists in  $\Omega$  and its shape is given by an inner boundary  $C_1$ .

author's e-mail: takayama@yz.yamagata-u.ac.jp

<sup>\*)</sup> This article is based on the presentation at the 22nd International Toki Conference (ITC22).

Throughout the present study, we adopt the Cartesian coordinate system  $\langle O : \mathbf{e}_x, \mathbf{e}_y, \mathbf{e}_z \rangle$ , where  $z$ -axis is parallel to the thickness direction. The origin  $O$  is chosen at the center of an HTS upper surface. In addition, the unit vectors along the  $x$ -,  $y$ - and  $z$ -directions are denoted by  $\mathbf{e}_x$ ,  $\mathbf{e}_y$  and  $\mathbf{e}_z$ , respectively. We assume that a vertical section of the coil is given by  $r_1 \leq r \leq r_2$  and  $z_1 \leq z \leq z_2$  with the cylindrical coordinates  $(r, \theta, z)$ . In order to determine the coil position, the symmetrical axis of the coil is shown by  $(x, y) = (x^*, y^*)$ .

According to the experimental results, the YBCO superconductors have a strong crystallographic anisotropy: the current flow in the  $c$ -axis direction differs from that in the  $ab$ -plane, and the flow along  $c$ -axis is almost negligible. Here, the  $c$ -axis is the direction along  $z$ , and it is perpendicular to the  $ab$ -plane. On the basis of the fact, we assume the thin-layer approximation [6]: the thickness of the HTS film is sufficiently thin that the shielding current density  $\mathbf{j}$  can hardly flow in the thickness direction.

A shielding current density  $\mathbf{j}$  is closely related to an electric field  $\mathbf{E}$ . The relation can be written as

$$\mathbf{E} = E(|\mathbf{j}|) \left( \frac{\mathbf{j}}{|\mathbf{j}|} \right), \quad (1)$$

where a function  $E(j)$  is given by the power law:

$$E(j) = E_C \left( \frac{j}{j_C} \right)^N. \quad (2)$$

Here,  $E_C$  is the critical electric field, and  $N$  is a constant.

Under the above assumptions, the shielding current density  $\mathbf{j}$  can be written as  $\mathbf{j} = (2/b)\nabla S \times \mathbf{e}_z$ , and the time evolution of the scalar function  $S(\mathbf{x}, t)$  is governed by the following integro-differential equation [6]:

$$\mu_0 \frac{\partial}{\partial t} (\hat{W}S) + \frac{\partial}{\partial t} (\mathbf{B} \cdot \mathbf{e}_z) + (\nabla \times \mathbf{E}) \cdot \mathbf{e}_z = 0, \quad (3)$$

where a bracket  $\langle \rangle$  denotes an average operator over the thickness of the film, and  $\mathbf{E}$  is an electro magnetic field. In addition,  $\hat{W}S$  is defined by

$$\hat{W}S \equiv \iint_{\Omega} Q(|\mathbf{x} - \mathbf{x}'|) S(\mathbf{x}', t) d^2\mathbf{x}' + (2/b)S(\mathbf{x}, t). \quad (4)$$

Here, both  $\mathbf{x}$  and  $\mathbf{x}'$  are position vectors in the  $xy$ -plane. The explicit form of  $Q(r)$  is described in [6].

$$Q(r) = -\frac{1}{\pi b^2} \left( \frac{1}{r} - \frac{1}{\sqrt{r^2 + b^2}} \right). \quad (5)$$

Note that  $Q(r)$  becomes singular at  $r = 0$ . Therefore, it is clearly necessary to evaluate the first right-hand side of (2) as an improper integral. Incidentally, the high-performance method of this integral is described in [7].

The initial and boundary conditions to (3) are assumed

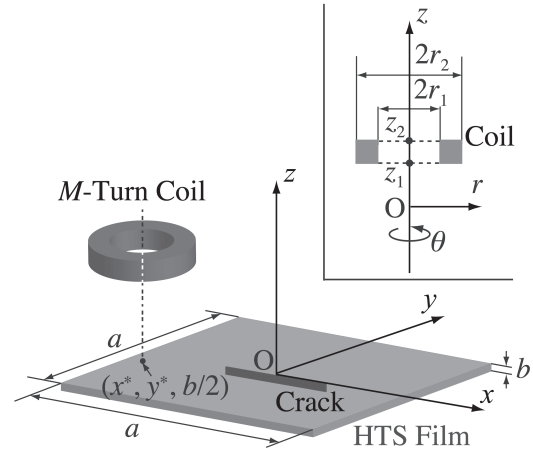


Fig. 1 A schematic view of an inductive method.

as follows:

$$S = 0 \text{ at } t = 0, \quad (6)$$

$$S = 0 \text{ on } C_0, \quad (7)$$

$$\frac{\partial S}{\partial s} = 0 \text{ on } C_1, \quad (8)$$

$$\oint_{C_1} \mathbf{E} \cdot \mathbf{t} ds = 0. \quad (9)$$

Here,  $s$  and  $\mathbf{t}$  denote an arclength along  $C_1$  and the tangential unit vector on  $C_1$ , respectively. By solving the initial-boundary-value problem of (3), we can determine the time evolution of the shielding current density in an HTS film.

Discretized with the backward Euler method, the initial-boundary-value problem of (3) is reduced to the nonlinear boundary-value problem. In order to solve the problem, we adopt the Newton method and the finite element method. On the basis of the numerical method, a numerical code has been developed for analyzing the shielding current density in an HTS film with a crack.

## 3. Simulation of Inductive Method

### 3.1 Mawatari's theory

According to Mawatari's theory [3], a critical current density  $j_C$  can be calculated from

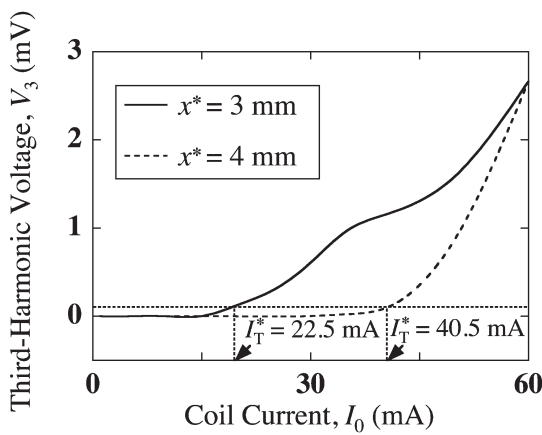
$$j_C^N = \frac{2F(r_{\max})I_T^*}{b}, \quad (10)$$

where  $j_C^N$  denotes an estimated value of  $j_C$ , and  $F(r_{\max})$  is the maximum value of a primary coil-factor function  $F(x)$  [3] determined from the configuration of the coil and the HTS.  $I_T^*$  is a lower limit of the coil current  $I_0$  when a third-harmonic voltage  $V_3$  begins to develop in the coil. An important point is that (10) is also applicable only to an HTS film without any cracks.

In order to simulate the inductive method, calculating a third-harmonic voltage  $V_3$  from time evolution of the shielding current density  $\mathbf{j}$ , we must determine an  $V_3$ - $I_0$  curve. For evaluating the value of  $I_T$ , we use the conven-

Table 1 The Geometrical and the physical parameters.

	Length	$a$	20 mm
	Thickness	$b$	600 nm
HTS Film	Critical current density	$j_c$	1 MA/cm <sup>2</sup>
	Critical electric field	$E_c$	1 mV/m
	$N$ -value of power law	$N$	20
	Number of turns	$M$	400
	Frequency	$f$	1 kHz
Coil	Bottom	$z_1$	0.2 mm
	Top	$z_2$	1.2 mm
	Inner radius	$2r_1$	2 mm
	Outer radius	$2r_2$	4 mm
	Maximum value of $F(x)$	$F_{\max}$	$7.28 \times 10^{-1}$


 Fig. 2  $V_3$ - $I_0$  curves for the case with  $L_c = 4$  mm and  $y^* = 0$  mm.

tional voltage criterion  $V_3 = 0.1$  mV  $\Leftrightarrow I_0 = I_T^*$  [3]. The numerical method of  $V_3$  is described in [7].

### 3.2 Detection of crack size and position

In this subsection, we investigate the applicability of the detection of a crack size and position by simulating the inductive method. Hereafter, we assume that a crack shape is a line segment parallel to  $x$ -axis. In addition, the center of crack position is denoted by  $(x, y) = (x_c, y_c)$  in the  $xy$ -plane, and the crack size is expressed as  $L_c$ . Values of the geometrical and the physical parameters used in the present study are tabulated in Table 1. In this study, the critical current density  $j_c$  is assumed to be homogeneous.

Firstly, we investigate the influence of the crack on a third-harmonic voltage  $V_3$ . In Fig. 2, we show the  $V_3$ - $I_0$  curves for various coil position  $L_c$ 's. We see from this figure that, beginning to develops drastically from a certain value of  $I_0$ , the third-harmonic voltage  $V_3$  increases with  $I_0$ . By applying the voltage criterion to the  $V_3$ - $I_0$  curve for  $x^* = 3$  mm, we get  $I_T^* = 22.5$  mA (see Fig. 2). This value is remarkably different from the analytic value  $I_T^A = 41.2$  mA of  $I_T$ . Incidentally,  $I_T^A$  can be calculated from the formula  $I_T^A = j_c b / [2F(r_{\max})]$  derived from (10). On the other hand, the value of  $I_T^*$  for  $x^* = 4$  mm is  $I_T^* = 40.5$  mA by using the

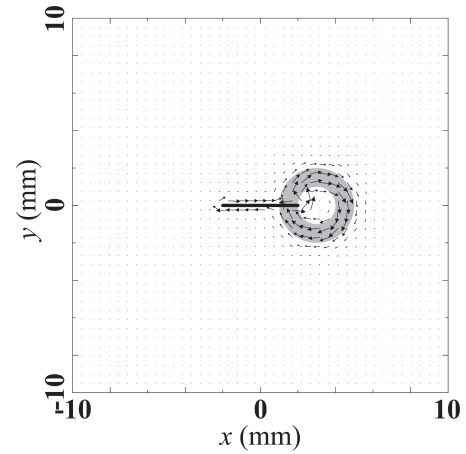
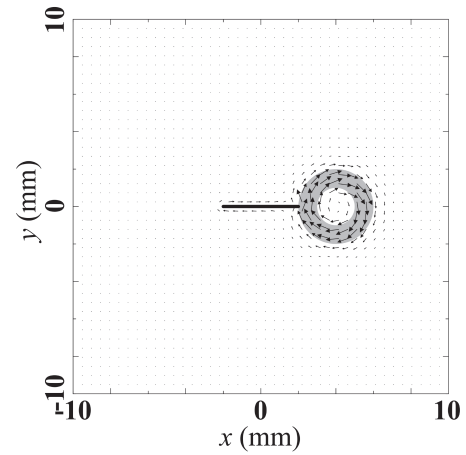

 (a)  $x^* = 3$  mm

 (b)  $x^* = 4$  mm

 Fig. 3 Spatial distributions of the shielding current density  $j$  at time  $ft = 1.2$ . Here,  $L_c = 4$  mm and  $y^* = 0$  mm.

voltage criterion.

Let us investigate the behavior of the shielding current density  $j$  for Fig. 2. In Figs. 3 (a) and (b), we show the spatial distributions of the shielding current density  $j$ . We see from this figure that, for  $x^* = 3$  mm, the spatial distribution of the shielding current density  $j$  is drastically disorder due to the crack. As a result, the distribution becomes asymmetry. On the other hand, for  $x^* = 4$  mm, the spatial distribution of  $j$  is almost symmetric about the symmetry axis of the coil because  $j$  hardly affects the crack. From these results, we imply that the crack size may be detected by using the inductive method.

Let us investigate the applicability of the detection of the crack size  $L_c$ . To this end, we define the relative error:

$$\varepsilon \equiv \frac{|j_c^N - j_c|}{j_c}. \quad (11)$$

Moreover, the symmetry axis of the coil is moved to  $x$ - and  $y$ -directions, and we examine the spatial distribution of the relative error  $\varepsilon$ . In Fig. 4, we show the dependence of the relative error  $\varepsilon$  on the coil position  $x^*$  for the case with  $L_c = 4$  mm and  $L_c = 8$  mm. This figure indicates that, for

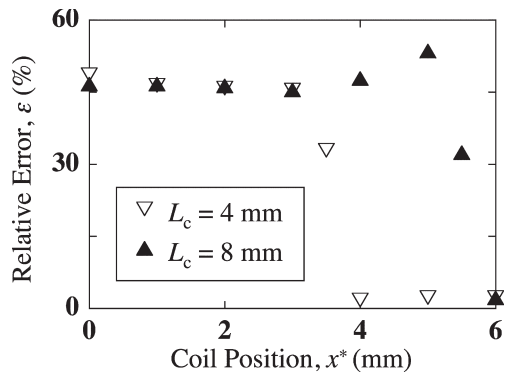


Fig. 4 Dependence of the relative error  $\varepsilon$  on the coil position  $x^*$  for the case with  $y^* = 0$  mm.

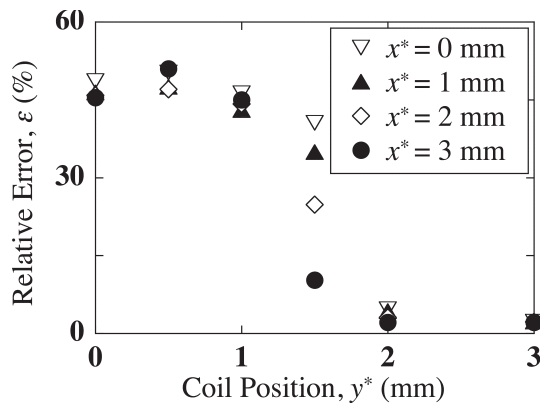


Fig. 5 Dependence of the relative error  $\varepsilon$  on the coil position  $y^*$  for the case with  $L_c = 4$  mm.

$L_c = 4$  mm, the relative error  $\varepsilon$  becomes remarkably large for  $x^* < 4$  mm. This case means that the orthographic projection of the coil overlaps with the crack (e.g. Fig. 3 (a)). In contrast, it is found that, for  $x^* > 4$  mm, the value of  $\varepsilon$  is almost constant, and the crack and the coil have in contact with each other at the point  $(x, y) = (4 \text{ mm}, 0 \text{ mm})$  (see Fig. 3 (b)). For  $L_c = 8$  mm, the value of  $\varepsilon$  is not less than 30% except for  $x^* = 6$  mm. This result shows a similar tendency to  $L_c = 4$  mm. Therefore, the orthographic projection of the coil significantly affects the accuracy of the inductive method.

Finally, the relative error  $\varepsilon$  is calculated as a function of the coil position  $y^*$  and is depicted in Fig. 5. We see from this figure that, for  $y^* < 2$  mm, the value of the relative error  $\varepsilon$  is not less than 10% regardless  $x^*$ , whereas  $\varepsilon$  is about 5% or less for  $y^* \geq 2$  mm. In Fig. 6, we show the spatial distribution of the shielding current density  $\mathbf{j}$  for  $x^* = y^* = 2$  mm. From this figure, although  $\mathbf{j}$  slightly flow along the crack, the spatial distribution of  $\mathbf{j}$  becomes roughly symmetry.

From these results, we conclude that if the orthographic projection of the coil overlaps with the crack, the accuracy of the inductive method is hardly degraded. Therefore, by measuring the spatial distribution of the critical current density  $j_c$ , the crack size and position can be detected accurately.

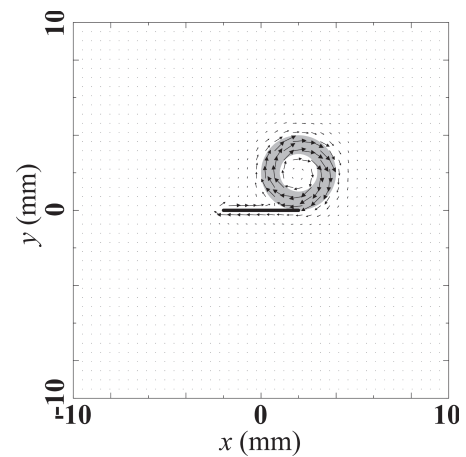


Fig. 6 Spatial distribution of the shielding current density  $\mathbf{j}$  at time  $ft = 1.2$ . Here,  $L_c = 4$  mm and  $x^* = y^* = 2$  mm.

## 4. Conclusion

We have developed a numerical code analyzing the time evolution of the shielding current density in an HTS film containing a crack. By using the code, reproducing the inductive method numerically, we assess the applicability of the detection of the crack size and position. Conclusions obtained in the present study are summarized as follows: if the orthographic projection of the coil overlaps with the crack, the accuracy of the inductive method is hardly degraded. This is mainly because the shielding current density flow on the region of the orthographic projection of the coil. Therefore, by measuring the spatial distribution of the critical current density, the crack size and position can be detected accurately.

## Acknowledgment

This work was supported in part by Japan Society for the Promotion of Science under a Grant-in-Aid for Scientific Research (B) No.22360042. A part of this work was carried out under the Collaboration Research Program (NIFS11KNTS011) at National Institute for Fusion Science (NIFS) Japan. In addition, the Numerical computations was carried out on Hitachi SR16000 XM1 of the LHD Numerical Analysis Server in NIFS.

- [1] B.P. Martins, *Recent Developments in Superconductivity Research* (Nova Publishers, New York, 2006) p. 68.
- [2] J.H. Claassen, M.E. Reeves and R.J. Soulen, Jr., *Rev. Sci. Instrum.* **62**, 996 (1991).
- [3] Y. Mawatari, H. Yamasaki and Y. Nakagawa, *Appl. Phys. Lett.* **81**, 2424 (2002).
- [4] S.B. Kim, *Physica C* **463-465**, 702 (2007).
- [5] T. Takayama, A. Kamitani and H. Hiroaki, *Plasma Fusion Res.* **7**, 2405017 (2012).
- [6] A. Kamitani and S. Ohshima, *IEICE Trans. Electron.* **E82-C**, 766 (1999).
- [7] T. Takayama and A. Kamitani, *IEEE Trans. Appl. Supercond.* **19**, 3573 (2009).